A bound-preserving upwind DG scheme for the convective Cahn-Hilliard model

Daniel Acosta Soba

Universidad de Cádiz
University of Tennessee at Chattanooga

J. Rafael Rodríguez Galván
(Universidad de Cádiz)

Francisco Guillén González
(Universidad de Sevilla)

BYMAT 2022

November 11, 2022

Section 1

Linear convection

Linear convection problem

We consider the linear convection problem:

$$\begin{aligned} v_t + \nabla \cdot (\boldsymbol{\beta} v) &= 0 && \text{in } \Omega \times (0, T), && \text{(1a)} \\ v(0) &= v_0 && \text{in } \Omega, && \text{(1b)} \end{aligned}$$

where

- $\boldsymbol{\beta} \colon \overline{\Omega} \to \mathbb{R}^d$ is continuous and incompressible, i.e, $\nabla \cdot \boldsymbol{\beta} = 0$ in Ω,
- $\boldsymbol{\beta} \cdot \boldsymbol{n} = 0$ on $\partial\Omega$.

Properties:

- Existence and uniqueness of the solution.
- Mass conservation: $\frac{d}{dt} \int_\Omega v = 0$.
- Maximum principle: $\min_{\overline{\Omega}} v_0 \leq v \leq \max_{\overline{\Omega}} v_0$ in $\overline{\Omega} \times (0, T)$.

Discontinuous Galerkin methods

$$\mathbb{P}_k^{\text{disc}}(\mathscr{T}_h) := \left\{ v_h \in L^2(\Omega) \colon v_{h|_{K_i}} \in \mathbb{P}_k(K_i) \text{ with } K_i \in \mathscr{T}_h, \forall i \in \{1, 2, \ldots, N_{\mathscr{T}_h}\} \right\}$$

with a basis $\{\phi_i\}_{i \in \{1,2,\ldots,N_h\}}$.

Notation:

- Average: $\{\!\{v\}\!\} := \begin{cases} \dfrac{v_K + v_L}{2} & \text{if } e = \partial K \cap \partial L \in \mathscr{E}_h^i \\ v_K & \text{if } e = \partial K \in \mathscr{E}_h^b \end{cases},$
- Jump: $[\![v]\!] := \begin{cases} v_K - v_L & \text{if } e = \partial K \cap \partial L \in \mathscr{E}_h^i \\ v_K & \text{if } e = \partial K \in \mathscr{E}_h^b \end{cases},$
- Positive part: $v_\oplus := \dfrac{|v| + v}{2} = \max\{v, 0\},$
- Negative part: $v_\ominus := \dfrac{|v| - v}{2} = -\min\{v, 0\},$
- $v = v_\oplus - v_\ominus$.

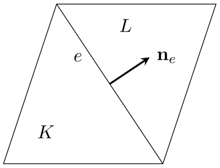

Figure: Orientation of unit normal vector.

DG upwind method

- $a_h^{\text{upw}} : \mathbb{P}_k^{\text{disc}}(\mathscr{T}_h) \times \mathbb{P}_k^{\text{disc}}(\mathscr{T}_h) \to \mathbb{R}$,

$$a_h^{\text{upw}}(\boldsymbol{\beta}; v, \overline{v}) := -\sum_{K \in \mathscr{T}_h} \int_K v(\boldsymbol{\beta} \cdot \nabla \overline{v}) + \sum_{e \in \mathscr{E}_h^i, e = K \cap L} \int_e \left((\boldsymbol{\beta} \cdot \boldsymbol{n}_e)_\oplus v_K - (\boldsymbol{\beta} \cdot \boldsymbol{n}_e)_\ominus v_L \right) [\![\overline{v}]\!]$$

Properties of the scheme for $k = 0$

Given $v^m \in \mathbb{P}_0^{\text{disc}}(\mathscr{T}_h)$, find $v^{m+1} \in \mathbb{P}_0^{\text{disc}}(\mathscr{T}_h)$ such that

$$\left(\frac{v^{m+1} - v^m}{\Delta t}, \overline{v}\right)_{L^2(\Omega)} + a_h^{\text{upw}}(\boldsymbol{\beta}; v^{m+1}, \overline{v}) = 0$$

for every $\overline{v} \in \mathbb{P}_0^{\text{disc}}(\mathscr{T}_h)$.

Properties:

- Existence and uniqueness of the solution.
- Mass conservation: $\int_\Omega v^{m+1} = \int_\Omega v^m$.
- Maximum principle: $\min_{\overline{\Omega}} v^m \le v^{m+1} \le \max_{\overline{\Omega}} v^m$ in $\overline{\Omega}$.

Section 2

Convective Cahn-Hilliard model

Cahn-Hilliard equation

Fourth order problem:

$$
\begin{aligned}
u_t &= \nabla \cdot \left(M(u) \nabla \left(-\varepsilon^2 \Delta u + F'(u) \right) \right) && \text{in } \Omega \times (0, T), \\
\nabla u \cdot \mathrm{n} &= \nabla(-\varepsilon^2 \Delta u + F'(u)) \cdot \mathrm{n} = 0 && \text{on } \partial\Omega \times (0, T), \\
u(0) &= u_0 && \text{in } \Omega.
\end{aligned}
$$

- $F(u) = \frac{1}{4} u^2 (1-u)^2$ Ginzburg-Landau double well functional.
- $M(u) = u(1-u)$ degenerate mobility function.
- u minimizes energy functional:

$$
E(u(t)) := \frac{\varepsilon^2}{2} \int_\Omega |\nabla u(t)|^2 dx + \int_\Omega F(u(t)) dx.
$$

- Applications: tumor tissues, image processing, multi-phase fluid systems, etc.

Convective Cahn-Hilliard model

$$\begin{aligned}
\partial_t u &= \nabla \cdot (M(u)\nabla\mu) - \nabla\cdot(u\boldsymbol{v}) && \text{in } \Omega\times(0,T),\\
\mu &= F'(u) - \varepsilon^2\Delta u && \text{in } \Omega\times(0,T),\\
\nabla u\cdot\boldsymbol{n} &= (M(u)\nabla\mu - u\boldsymbol{v})\cdot\boldsymbol{n} = 0 && \text{on } \partial\Omega\times(0,T),\\
u(0) &= u_0 && \text{in } \Omega.
\end{aligned}$$

where

- $\boldsymbol{v} : \overline{\Omega}\times(0,T)\to\mathbb{R}^d$ is continuous and incompressible, i.e, $\nabla\cdot\boldsymbol{v} = 0$ in Ω,
- $\boldsymbol{v}\cdot\boldsymbol{n} = 0$ on $\partial\Omega$.

Properties:

- Mass conservation: $\frac{d}{dt}\int_\Omega u = 0$.
- Maximum principle: $u\in[0,1]$ in $\overline{\Omega}\times(0,T)$ if $u_0\in[0,1]$ in $\overline{\Omega}$.

Nonlinear flux direction

Notice that

$$\nabla \cdot (M(u)\nabla\mu) = M'(u)\nabla\mu \cdot \nabla u + M(u)\Delta\mu.$$

Hence, $M'(u)$ determines the direction of the flux.

- If $u \in [0,1]$ then $M(u) = M(u)_\oplus$.

Consider:

- Increasing part of $M(u)_\oplus$: $M^\uparrow(u) = \begin{cases} M(u)_\oplus & \text{if } u \leq \frac{1}{2} \\ M\left(\frac{1}{2}\right) & \text{if } u > \frac{1}{2} \end{cases}.$
- Decreasing part of $M(u)_\oplus$: $M^\downarrow(u) = \begin{cases} 0 & \text{if } u \leq \frac{1}{2} \\ M(u)_\oplus - M\left(\frac{1}{2}\right) & \text{if } u > \frac{1}{2} \end{cases}.$

Notice that $M(u)_\oplus = M^\uparrow(u) + M^\downarrow(u)$.

Generalized upwind method

- $a_h^{\text{upw}} : \mathbb{P}_k^{\text{disc}}(\mathscr{T}_h) \times \mathbb{P}_k^{\text{disc}}(\mathscr{T}_h) \to \mathbb{R}$,

$$a_h^{\text{upw}}(\boldsymbol{\beta}; M(u)_\oplus, \overline{u}) := -\int_\Omega (\boldsymbol{\beta} \cdot \nabla \overline{u}) M(u)_\oplus$$
$$+ \sum_{e \in \mathscr{E}_h^i, e = K \cap L} \int_e \Big((\{\!\{\boldsymbol{\beta}\}\!\} \cdot \boldsymbol{n}_e)_\oplus (M^\uparrow(u_K) + M^\downarrow(u_L))$$
$$-(\{\!\{\boldsymbol{\beta}\}\!\} \cdot \boldsymbol{n}_e)_\ominus (M^\uparrow(u_L) + M^\downarrow(u_K)) \Big) [\![\overline{u}]\!] ,$$

where $\boldsymbol{\beta} \colon \overline{\Omega} \to \mathbb{R}^d$ can be discontinuous over $\mathscr{E}_h^{\mathrm{i}}$.

Fully discrete scheme

Given $u^m \in \mathbb{P}_0^{\text{disc}}(\mathscr{T}_h)$ with $u^m \in [0,1]$, find $u^{m+1} \in \mathbb{P}_0^{\text{disc}}(\mathscr{T}_h)$, with $\mu^{m+1}, w^{m+1} \in \mathbb{P}_1^{\text{cont}}(\mathscr{T}_h)$, solving

$$\left(\frac{u^{m+1}-u^m}{\Delta t}, \overline{u}\right)_{L^2(\Omega)} + a_h^{\text{upw}}(-\nabla\mu^{m+1}; M(u^{m+1})_\oplus, \overline{u}) + a_h^{\text{upw}}(\boldsymbol{v}(t_{m+1}); u^{m+1}, \overline{u}) = 0,$$

$$\left(\mu^{m+1}, \overline{\mu}\right)_{L^2(\Omega)} = \varepsilon^2 \left(\nabla w^{m+1}, \nabla\overline{\mu}\right)_{L^2(\Omega)} + \left(f(u^{m+1}, u^m), \overline{\mu}\right)_{L^2(\Omega)},$$

$$\left(w^{m+1}, \overline{w}\right)^h_{L^2(\Omega)} = \left(u^{m+1}, \overline{w}\right)_{L^2(\Omega)},$$

for all $\overline{u} \in \mathbb{P}_0^{\text{disc}}(\mathscr{T}_h)$ and $\overline{\mu}, \overline{w} \in \mathbb{P}_1^{\text{cont}}(\mathscr{T}_h)$.

$(\cdot,\cdot)^h_{L^2(\Omega)}$ denotates the scalar product with mass-lumping.

Properties:

- Existence of a solution.
- Mass conservation: $\int_\Omega u^{m+1} = \int_\Omega u^m$, $\int_\Omega w^{m+1} = \int_\Omega w^m$.
- Maximum principle: $u^{m+1}, w^{m+1} \in [0,1]$ in $\overline{\Omega}$ if $u^m, w^m \in [0,1]$.

Section 3

Numerical tests

Non-convective Cahn-Hilliard ($\boldsymbol{v} = 0$)

FEM

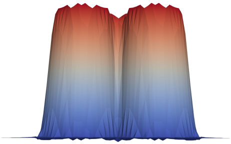

DG-SIP

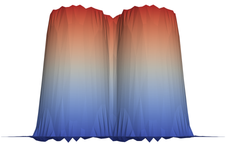

DG-UPW

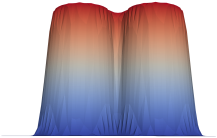

Convective Cahn-Hilliard with FEM ($\boldsymbol{v} = 100(y, -x)$)

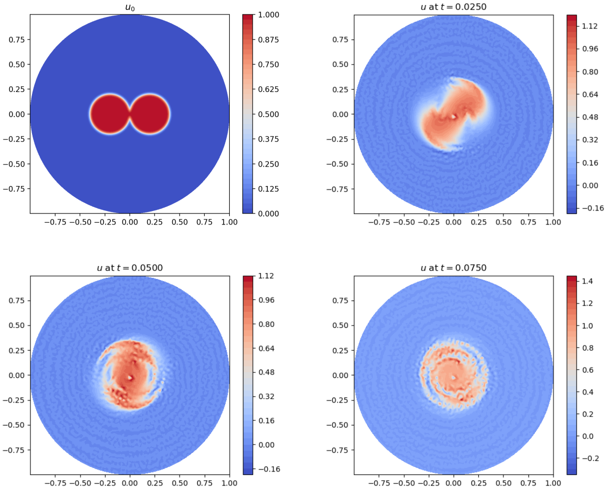

Convective Cahn-Hilliard with DG-SIP ($\boldsymbol{v} = 100(y, -x)$)

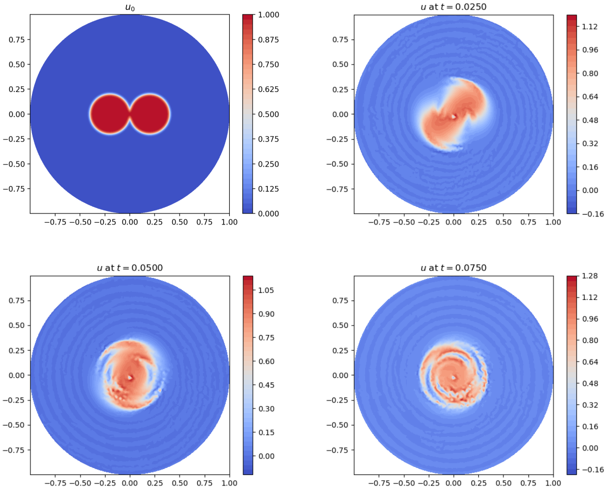

Convective Cahn-Hilliard with DG-UPW ($\boldsymbol{v} = 100(y, -x)$)

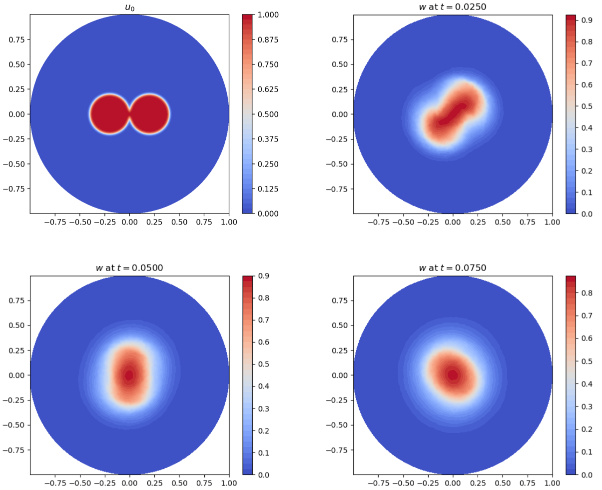

Convective Cahn-Hilliard ($\boldsymbol{v} = 100(y, -x)$)

Maximum-Minimum

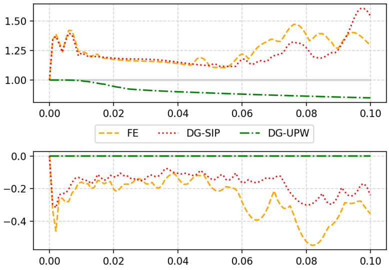

Dynamics

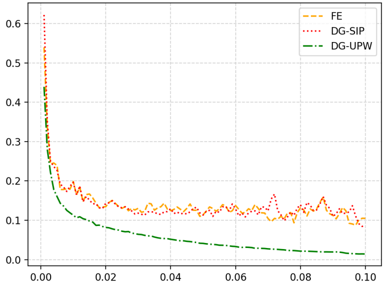

Figure: On the left, maximum and minimum of the phase field variable over time. On the right, we plot $\frac{\left\| u^{m+1} - u^m \right\|_{L^\infty(\Omega)}}{\left\| u^m \right\|_{L^\infty(\Omega)}}$ to observe the dynamics of the approximations.

Stokes-Cahn-Hilliard with FEM (cavity test)

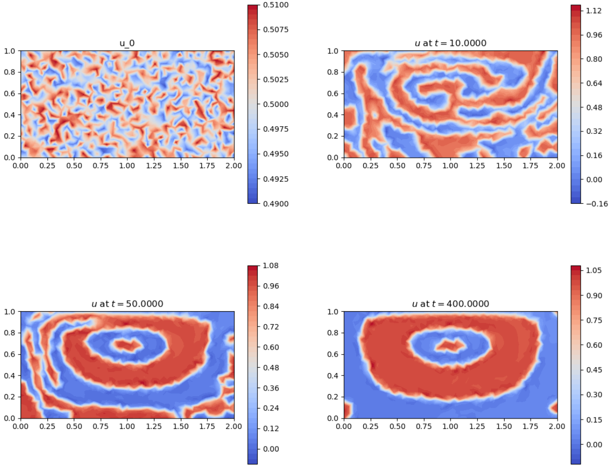

Stokes-Cahn-Hilliard with DG-SIP (cavity test)

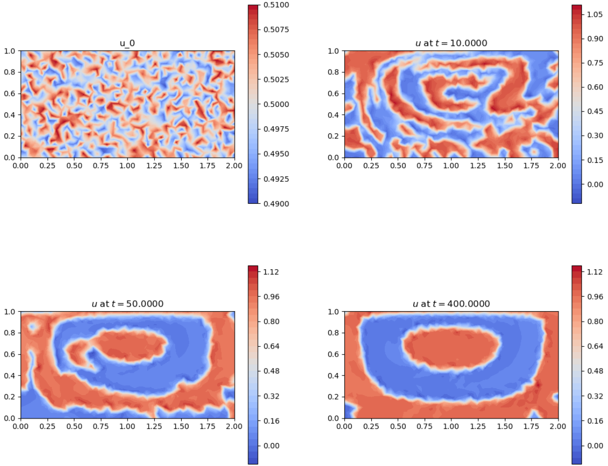

Stokes-Cahn-Hilliard with DG-UPW (cavity test)

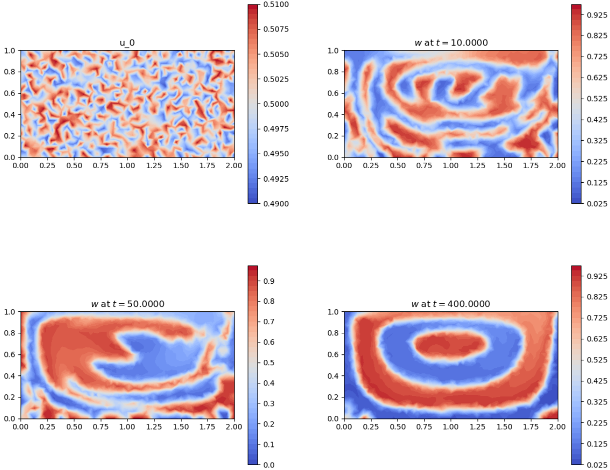

Stokes-Cahn-Hilliard (cavity test)

Maximum-Minimum

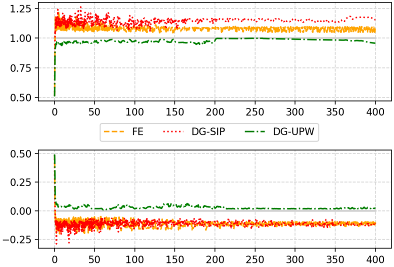

Dynamics

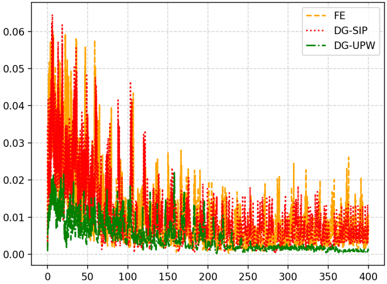

Figure: On the left, maximum and minimum of the phase field variable over time. On the right, we plot $\frac{\left\| u^{m+1} - u^m \right\|_{L^\infty(\Omega)}}{\left\| u^m \right\|_{L^\infty(\Omega)}}$ to observe the dynamics of the approximations.

Convergence order: non-convective Cahn-Hilliard

Table: Errors and convergence orders at $T = 0.001$ without convection ($\boldsymbol{v} = 0$).

Scheme	Norm	$h \approx 2.8284 \cdot 10^{-2}$	$h/2 \approx 1.4142 \cdot 10^{-2}$		$h/3 \approx 9.428 \cdot 10^{-3}$		$h/4 \approx 7.071 \cdot 10^{-3}$	
		Error	Error	Order	Error	Order	Error	Order
DG-UPW	$\|\cdot\|_{L^2}$	$8.5268 \cdot 10^{-3}$	$3.0933 \cdot 10^{-3}$	1.46	$1.7645 \cdot 10^{-3}$	1.38	$1.2134 \cdot 10^{-3}$	1.30
	$\|\cdot\|_{H^1}$	$8.0000 \cdot 10^{-1}$	$4.0199 \cdot 10^{-1}$	0.99	$2.6081 \cdot 10^{-1}$	1.07	$1.8849 \cdot 10^{-1}$	1.13
FEM	$\|\cdot\|_{L^2}$	$5.3224 \cdot 10^{-3}$	$1.5679 \cdot 10^{-3}$	1.76	$6.9944 \cdot 10^{-4}$	1.99	$4.0191 \cdot 10^{-4}$	1.93
	$\|\cdot\|_{H^1}$	$8.9963 \cdot 10^{-1}$	$4.1080 \cdot 10^{-1}$	1.13	$2.5252 \cdot 10^{-1}$	1.2	$1.7799 \cdot 10^{-1}$	1.22
DG-SIP	$\|\cdot\|_{L^2}$	$4.6466 \cdot 10^{-3}$	$1.3023 \cdot 10^{-3}$	1.84	$5.8945 \cdot 10^{-4}$	1.96	$3.2710 \cdot 10^{-4}$	2.05
	$\|\cdot\|_{H^1}$	1.1784	$5.8331 \cdot 10^{-1}$	1.01	$3.6254 \cdot 10^{-1}$	1.17	$2.6024 \cdot 10^{-1}$	1.15

Convergence order: convective Cahn-Hilliard

Table: Errors and convergence orders at $T = 0.001$ with convection ($\boldsymbol{v} = (y, -x)$).

Scheme	Norm	$h \approx 4 \cdot 10^{-2}$	$h/2 \approx 2 \cdot 10^{-2}$		$h/3 \approx 1.3333 \cdot 10^{-2}$		$h/4 \approx 1 \cdot 10^{-2}$	
		Error	Error	Order	Error	Order	Error	Order
DG-UPW	$\lVert\cdot\rVert_{L^2}$	$1.7288 \cdot 10^{-2}$	$6.9446 \cdot 10^{-3}$	1.32	$3.3102 \cdot 10^{-3}$	1.83	$2.0578 \cdot 10^{-3}$	1.65
	$\lVert\cdot\rVert_{H^1}$	1.4549	$6.0305 \cdot 10^{-1}$	1.27	$3.0204 \cdot 10^{-1}$	1.71	$2.0315 \cdot 10^{-1}$	1.38
FEM	$\lVert\cdot\rVert_{L^2}$	$6.8347 \cdot 10^{-3}$	$2.1213 \cdot 10^{-3}$	1.69	$9.7749 \cdot 10^{-4}$	1.91	$5.3883 \cdot 10^{-4}$	2.07
	$\lVert\cdot\rVert_{H^1}$	$8.3104 \cdot 10^{-1}$	$3.8060 \cdot 10^{-1}$	1.13	$2.1887 \cdot 10^{-1}$	1.36	$1.4991 \cdot 10^{-1}$	1.32
DG-SIP	$\lVert\cdot\rVert_{L^2}$	$6.5242 \cdot 10^{-3}$	$1.9557 \cdot 10^{-3}$	1.74	$8.9471 \cdot 10^{-4}$	1.93	$5.0257 \cdot 10^{-4}$	2.00
	$\lVert\cdot\rVert_{H^1}$	1.1980	$6.1624 \cdot 10^{-1}$	0.96	$3.8451 \cdot 10^{-1}$	1.16	$2.7439 \cdot 10^{-1}$	1.17

References

Acosta-Soba, D., Guillén-González, F., and Rodríguez-Galván, J. R. (2022).
An upwind DG scheme preserving the maximum principle for the convective Cahn–Hilliard model.
Numerical Algorithms.

Di Pietro, D. A. and Ern, A. (2012).
Mathematical Aspects of Discontinuous Galerkin Methods.
Springer, Berlin; New York.

Frank, F., Liu, C., Alpak, F. O., and Riviere, B. (2018).
A finite volume / discontinuous Galerkin method for the advective Cahn–Hilliard equation with degenerate mobility on porous domains stemming from micro-CT imaging.
Computational Geosciences, 22(2):543–563.

Hawkins-Daarud, A., van der Zee, K. G., and Tinsley Oden, J. (2012).
Numerical Simulation of a Thermodynamically Consistent Four-Species Tumor Growth Model.
International Journal for Numerical Methods in Biomedical Engineering, 28(1):3–24.

Ibrahim, M. and Saad, M. (2014).
On the efficacy of a control volume finite element method for the capture of patterns for a volume-filling chemotaxis model.
Computers & Mathematics with Applications, 68(9):1032–1051.

Thanks for your attention!

Acknowledgements

The speaker has been supported by a *Graduate Scholarship funded by the University of Tennessee at Chattanooga* and by *UCA FPU contract UCA/REC14VPCT/2020 funded by Universidad de Cádiz*. The collaborators have been supported by *Grant PGC2018-098308-B-I00* by *MCI N/AEI/ 10.13039/501100011033* and by *ERDF a way of making Europe*.